Synthesis of Fe-doped ZnO nanoparticles using *Coriandrum sativum* extract for degradation of Congo-Red dye

Dissertation submitted to
Visvesvaraya National Institute of Technology, Nagpur
in partial fulfillment of the requirements for the award of the degree

of

Master of Technology
in
Chemical Engineering

by

Samiksha Dhole (MT23MCL006)

under the guidance of
Dr. Arijit Das

Department of Chemical Engineering
Visvesvaraya National Institute of Technology
Nagpur 440 010 (India)

June, 2025

Synthesis of Fe-doped ZnO nanoparticles using *Coriandrum sativum* extract for degradation of Congo-Red dye

Dissertation submitted to
Visvesvaraya National Institute of Technology, Nagpur
in partial fulfillment of the requirements for the award of the degree

of

Master of Technology
in
Chemical Engineering

by

Samiksha Dhole (MT23MCL006)

under the guidance of
Dr. Arijit Das

Department of Chemical Engineering
Visvesvaraya National Institute of Technology
Nagpur 440 010 (India)

June, 2025

© Visvesvaraya National Institute of Technology (VNIT) 2025

Department of Chemical Engineering
Visvesvaraya National Institute of Technology, Nagpur

Declaration

I, **Samiksha Dhole,** hereby declare that this dissertation titled **"Synthesis of Fe-doped ZnO nanoparticles using *coriandrum sativum* extract for degradation of Congo-Red dye**" is carried out by me in the Department of **Chemical Engineering** of **Visvesvaraya National Institute of Technology, Nagpur.** The work is original and has not been submitted earlier whole or in part for the award of any degree/diploma at this or any other Institution / University.

Samiksha Dhole

Certificate

This to certify that the dissertation titled **"Synthesis of Fe-doped ZnO nanoparticles using coriandrum sativum extract for degradation of Congo-Red dye"** is submitted by **Samiksha Dhole** in partial fulfillment of the requirements for the award of the degree of **Master of Technology in Chemical**, VNIT Nagpur. The work is comprehensive, complete and fit for final evaluation.

Dr. Arijit Das
Associate Professor
Dept. of Chemical Engineering
VNIT, Nagpur

Dr. K. L. Wasewar
Professor and Head,
Department of Chemical Engineering
VNIT, Nagpur
Date:

Visvesvaraya National Institute of Technology, Nagpur

Non-Plagiarism Certificate

Certified that M. Tech dissertation titled **"Synthesis of Fe-doped ZnO nanoparticles using *coriandrum sativum* extract for degradation of Congo-Red dye"** Submitted by **Samiksha Dhole,** Enrolment No: **MT23MCL006**, ID No.: **30813** has been checked for plagiarism using, TURNITIN software and the overlap is found within prescribed limits. A summary of report is given below:

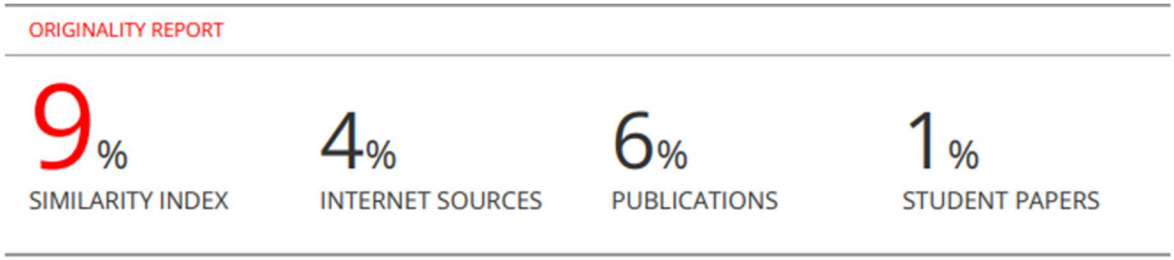

Signature

Student Name: **Samiksha Dhole**
Enrolment No.: **MT23MCL006**
ID No.: **30813**

Signature

Dr. Arijit Das

Associate Professor
Dept. of Chemical Engineering
VNIT, Nagpur

ACKNOWLEDGEMENT

I would like to express my heartfelt gratitude to my research guide, Dr. Arijit Das, for his invaluable guidance, constant support, and insightful feedback throughout the course of this thesis. His mentorship has been instrumental in shaping my research and academic development.

I am also deeply thankful to Dr. Dipak Giram, whose expertise, patience, and continuous encouragement played a crucial role in overcoming various challenges during the experimental and analytical phases of my work.

I extend my sincere thanks to Dr. Kailas Wasewar, Head of the Department of Chemical Engineering, for providing the necessary infrastructure, resources, and a conducive research environment that greatly contributed to the successful completion of my project.

I would also like to express my heartfelt gratitude to **Visvesvaraya National Institute of Technology, Nagpur,** for affording the infrastructural support, laboratory facilities, and academic ambiance through which this research was made possible.

Last but not least, I would like to thank my friends and classmates for their constant motivation, constructive discussions, and emotional support throughout this journey

Samiksha Dhole

MT23MCL006

ABSTRACT

The present study is focused on green synthesis of iron doped zinc oxide (ZnO) nanoparticles by *Coriandrum sativum* (coriander) leaf extract and photocatalytic use for Congo-red dye degradation. Traditional methods for the preparation of nanoparticles can involve toxic chemicals and are energy demanding, whereas green synthesis has an environmentally friendly, low-cost, and green process.

In this work, the leaf extract of coriander serves as a reducing and stabilizing agent to allow the synthesis of Fe-doped ZnO nanoparticles under mild conditions. The doped nanoparticles were characterized by several analytical methods. X-ray diffraction analysis confirmed that the nanoparticles were crystalline in nature, where characteristic peaks assured the successful doping of Fe into ZnO lattice. The presence of Zn–O and Fe–O bonds was confirmed by Fourier-transform infrared spectroscopy, indicating the structural integrity of doped nanoparticles.

This work emphasizes the viability of employing plant-mediated synthesis in developing advanced functional nanomaterials for engineering and offers a green solution to effluents contaminated with dyes. The suggested mechanism depicts the formation of reactive oxygen species, *i.e.*, hydroxyl radicals (•OH), which are responsible for the degradation process. This green synthesis pathway not only meets environmental safety standards but also promotes the development of efficient and low-cost photocatalysts for practical applications.

Keywords: *Green synthesis*, *Nanomaterials*, *Doping*, *Photocatalysis*, *Congo-red dye*, *Degradation*

INDEX

ABSTRACT ..... **i**

INDEX ..... **ii**

LIST OF FIGURES ..... **iv**

LIST OF TABLES ..... **vi**

NOMENCLATURE ..... **vii**

ABBREVIATIONS ..... **viii**

CHAPTER 1: INTRODUCTION **1**

1.1 Background 1

1.2 Motivation for the Research 3

1.3 Objectives of the Research 4

CAPTER 2: LITERATURE REVIEW **6**

2.1 Textile Dye Pollution 6

2.2 Overview of Congo Red and Dye Pollution 7

2.3 Green synthesis of ZnO photocatalyst 8

2.4 Mechanism of Fe doped ZnO photocatalyst 11

CHAPTER 3: MATERIALS AND EXPERIMENTAL METHODS **14**

3.1 Introduction 14

3.2 Materials 14

3.3 Experimental Methods 14

3.3.1 Preparation of plant Extract 14

3.3.2 Green Synthesis of Fe-Doped ZnO Nanoparticles 15

3.4 Photocatalytic activity of Congo Red dye degradation 16

3.5 Characterization 17

CHAPTER 4: RESULTS AND DISCUSSIONS 18
4.1 Characterization of ZnO and Iron doped ZnO nanoparticles 18
4.3.1 XRD diffraction analysis 18
4.3.2 Fourier Transform Infrared Analysis 21
4.3.3 FESEM and EDS analysis 22
4.2 Photocatalytic activity 23
4.2.1 Effect of Contact Time 23
4.2.2 Effect of Catalyst Dosage 24
4.2.3 Effect of Dye Concentrate 25
4.3 Kinetic study on photocatalytic degradation 28
4.4 Mechanism of dye degradation 29
4.5 Conclusion 30

CHAPTER 5: SUMMARY, KEY CONCLUSIONS, AND RECOMMENDATIONS FOR FUTURE WORK 31
5.1 Summary of Work 31
5.2 Key Conclusions 32
5.3 Limitations of Study 32
5.4 Future Perspectives 32

LIST OF FIGURES

Fig. No.	Title	Page
Fig 3.1	Experimentation Setup	15
Fig 3.2	Fe-doped ZnO nanoparticles	16
Fig 4.1	XRD analysis of Pure ZnO	19
Fig 4.2	XRD analysis of Fe-doped ZnO	20
Fig 4.3	XRD spectrum of Pure ZnO and Fe-doped ZnO	20
Fig 4.4	FTIR analysis of Fe-doped ZnO	21
Fig 4.5	FESEM analysis of Pure ZnO and Fe-doped ZnO	22
Fig 4.6	Illustrates the influence of irradiation time on the degradation efficiency of Congo Red-dye using Fe-doped ZnO nanoparticles. The experiment was conducted with a photocatalyst dose of 200 mg, an initial dye concentration of 30 ppm, and solution pH of 7.	23
Fig 4.7	Shows the impact of varying catalyst dosages on the degradation of Congo Red dye using Fe-doped ZnO nanoparticles. The study was carried out with a dye concentration of 30 ppm, a contact time of 120 minutes, and a pH of 7.	24
Fig 4.8	Illustrates how varying the initial concentration of Congo Red dye affects its degradation using Fe: ZnO nanoparticles. The experiment was conducted under controlled conditions with a 300 mg catalyst dosage, 120 minutes of irradiation, and a neutral pH of 7.	25
Fig 4.9	Illustrates the impact of solution pH on the degradation efficiency of Congo Red dye utilizing Fe:ZnO nanoparticles. The study was carried out with a contact time of 120 minutes, a catalyst amount of 300 mg, and an initial dye concentration of 10 ppm.	26

Fig. No.	Title	Page
Fig 4.10	Demonstrates how different Fe doping levels influence the degradation of Congo Red dye using Fe: ZnO nanoparticles. The experiment was performed with a photocatalyst dosage of 300 mg, initial dye concentration of 10 ppm, pH 3, and an irradiation period of 120 minutes	27
Fig 4.11	Depicts the pseudo-first-order kinetic plot for the degradation of Congo Red dye facilitated by Fe:ZnO nanoparticles.	28

LIST OF TABLES

Table No.	Title	Page
Table 3.1	List of the chemical reagents used for the experimental work	14

NOMENCLATURE

Symbol	Description	Unit
D	Average crystallite size	nm
K	Shape factor (typically 0.9)	Dimensionless
λ	X-ray wavelength	nm
β	Full width at half maximum (FWHM) of the peak	radians
θ	Bragg angle	radians
C_o	Initial dye concentration	mg/L (or ppm)
C_t	Final dye concentration after irradiation	mg/L (or ppm)
k	Rate constant (pseudo-first-order reaction)	min^{-1}

ABBREVIATIONS

Abbreviation	Full Form
XRD	X-ray Diffraction
FTIR	Fourier Transform Infrared Spectroscopy
FESEM	Field Emission Scanning Electron Microscopy
EDS	Energy Dispersive Spectroscopy
UV-Vis	Ultraviolet–Visible Spectroscopy
ROS	Reactive Oxygen Species
PZC	Point of Zero Charge
NPs	Nanoparticles
AOPs	Advanced Oxidation Processes
CB	Conduction Band
VB	Valence Band
CR	Congo Red

CHAPTER 1: INTRODUCTION

1.1 Background

A massive threat to the eco is the ongoing discharge of synthetic dyes into water bodies from textile and other dye-using industries Among these dyes, Congo red, an anionic azo dye, is particularly concerning. It is attributed to its strong solubility in water, chemically stable, and high resistance to biodegradation. Its persistence in aquatic environments not only hampers sunlight penetration and photosynthetic activity but also introduces carcinogenic and mutagenic risks to aquatic life and humans alike.

Conventional wastewater treatment methods like coagulation, filtration, and biological degradation have had trouble eliminating complex color compounds. Therefore, developing cutting-edge, effective, and environmentally responsible methods to break down synthetic dyes is what is needed the most now.

The possibility for full mineralization of organic contaminants under light irradiation has drawn a lot of interest to photocatalysis employing semiconductor metal oxides in recent years. Zinc oxide (ZnO) is recognized for its photocatalytic abilities owing to its wide energy band gap, high electron transport capability, and chemical robustness. However, the actual applications of pure ZnO are limited because to its limitations, which include low absorption of visible light and quick recombination of photogenerated electrons and holes.

A decrease in band gap energy, increased charge separation, and an introduction of dopants facilitates an extension of the material's light absorption capability into the visible spectrum., doping ZnO with transition metals such as iron (Fe) has been shown to enhance its light-driven catalytic efficiency in a bid to overcome these limitations. Using Plant-mediated nanoparticle synthesis has proved as a viable alternative to traditional chemical and physical processes. Plant extracts as reducing and stabilizing agents has proved to be non-toxic, energy-efficient, and eco-friendly. With regard to this, the easily available culinary spice coriander, Coriandrum sativum contains valuable bioactive constituents like

flavonoids, phenols, and terpenes is abundant of bio-resource for the fabrication of nanoparticles.

The rapid expansion of industrialization, especially in the textile industry, has resulted in large-scale application of synthetic dyes like Congo red, which are highly hazardous to aquatic life and human health owing to their toxic, carcinogenic, and persistent properties [1], [2], [3]. Conventional treatments used for wastewater treatment fail to degrade such large and complex organic dye molecules entirely, resulting in the need for alternative more efficient, green, and advanced remediation approaches [4], [5].

Among several advanced oxidation processes, semiconductor-based photocatalysis has been an encouraging method for the degradation of dye contaminants in aqueous systems based on its efficiency, cost-effectiveness, and low secondary pollution [6], [7], [8]. Zinc oxide (ZnO), being characterized by a large energy band gap, significant exciton binding energy along with high photocatalytic efficiency, has gained significant interest for photocatalytic uses [9], [10]. Nevertheless, its fast electron-hole recombination and low activity under visible light make it difficult to apply practically.

To overcome these constraints, different strategies including doping with transition metals (e.g., Fe, Cu) and creating nanocomposites have been employed to improve the visible-light response and separate the photogenerated charge carriers in ZnO [11], [12], [13], [14], [15]. Introducing Fe into ZnO reduces its band gap, enhances its visible light responsiveness, and significantly boosts its dye degradation efficiency. [13], [14], [16]

Concurrently, the development of greensynthesis pathways towards nanoparticle product ion has been gaining increased attention as they inherit abilities serving dual roles as reducers and capping agents. These green procedures avoid the usage of toxic chemicals and thus render the process more sustainable [9], [17], [18], [19], [20]. Different plant-mediated syntheses of ZnO nanoparticles have been synthesized using Neem [19], Amaranthus spinosus [21], Psidium guajava [17], Pomegranate peel [22], and Coriandrum sativum [18] and have been found to exhibit promising outcomes in both structural stability and photocatalytic activities.

leaf extract derived from Coriandrum sativum (commonly known as coriander), in fact, has been found to be capable of producing stable ZnO nanoparticles with optimal optical properties [18]. Still, not many studies incorporate Fe doping as part of coriander-mediated

green synthesis for the decomposition via photocatalysis of recalcitrant dyes such as Congo red. Although there are reports of Congo red degradation success in other green ZnO-based systems [6], [7], [8], [23], [24], the synergistic role of Fe doping and coriander extract-mediated synthesis for this particular application is not well explored.

Therefore, the current thesis focuses on the synthesis in a green way of Iron-doped ZnO nanoparticles developed through the use of leaf extract of Coriandrum sativum, along with their structural, optical, and photocatalytic characterization for the decomposition of CR dye molecules under photocatalytic conditions. This study aims to bridge a significant research gap by integrating the eco-friendly approach of plant-mediated synthesis with the enhanced functionality imparted by Fe doping, to develop efficient and sustainable photocatalysts for wastewater treatment.

1.2 Motivation for the Research

Uncontrolled release of dye-stuffed wastewater from allied and textile industries has become a critical environmental problem, degrading aquatic biodiversity and causing severe human health hazards [1], [2], [3]. Congo red, an azo dye that is popular in the textile industry, is not biodegradable, carcinogenic, and extremely toxic, which has led to its removal from wastewater gaining environmental importance [4], [6], [7], [23].

Conventional treatment processes like coagulation, filtration, and adsorption prove to be insufficient for the total degradation of synthetic dyes like Congo red, particularly under economically favorable and environmentally sustainable conditions [5], [8]. Semiconductor photocatalysis has thus picked up pace as it can degrade organic contaminants into innocuous end products under exposure to light irradiation [6], [25], [23].

ZnO nanoparticles have also shown great potential as photocatalysts owing to their electron mobility, high surface area, and non-toxicity [9], [10]. Pristine ZnO suffers from a wide band gap and high electron-hole recombination, which decreases its light-driven catalytic efficiency under visible light [9], [11].

Concurrently with the development of technologies, the application of green synthesis pathways for fabricating nanoparticles is also gaining growing interest because of their

sustainability, safety, and lower environmental impact [9], [21], [17], [16], [18]. Green synthesis via plant-mediated synthesis is a natural and environmentally benign pathway where phytochemicals act as reducing as well as capping agents. Many research studies have utilized plant extracts such as Amaranthus spinosus [14], Psidium guajava [15], Pomegranate peel [16], and Coriandrum sativum [18] for ZnO nanoparticle synthesis with stable and good light-driven catalytic efficiency.

To counter these limitations, researchers have doped ZnO with Metals like iron, copper, and cobalt to modulate its band structure and improve light-driven catalytic efficiency [11], [12], [13], [14], [15]. Of these, Fe doping has produced dramatic improvements in the separation of charge carriers and absorption in visible light and is therefore a very promising strategy [26].

Notwithstanding these developments, no studies that integrate Fe doping with Coriandrum sativum green synthesis to degrade Congo red dye have been reported. Coriandrum sativum is abundantly available, rich in phenolics and flavonoids, yet underutilized for the synthesis of high-performance photocatalyst materials [18]. The potential for synergistic integration between green chemistry concepts and nanotechnology for cleaning up the environment is a compelling reason for this research.

Thus, this study is motivated by the imperative to create a low-cost, highly efficient, and sustainable photocatalyst by synthesizing Coriandrum sativum leaf extract-mediated Fe-doped ZnO nanoparticles. The intention is to support the world's drive to counter dye pollution using an economically viable and environmentally sustainable process.

1.3 Objectives of the Research

The objective of this study is to examine the dye’s breakdown behavior of Fe doped ZnO which is synthesized via green synthesis method using coriander plant for Congo Red dye high-mast poles caused by wind with a blend of numerical and computational methods with attention to critical conditions that will result in structural collapse as a result of vortex-induced vibrations and stress concentration of interference-fitted joints.

To attain this, the particular research objectives are as follows:

1. In order to carry out the photocatalysis of ZnO, ZnO was first synthesized via green synthesis using coriander leaf extract. Iron (Fe) was then doped into the ZnO to evaluate the enhancement in degradation efficiency, which plays an important role in dye degradation.

2. A number of material characterization techniques was utilized to better understand the properties of the synthesized nanoparticles. These employed Scanning Electron Microscopy (SEM) to study the surface morphology surface morphology, to identify FTIR was used to detect functional groups, and XRD characterized the crystalline phases.to analyze the crystal structure, and UV-visible spectroscopy to evaluate optical behavior.

3. To assess their influence on the effectiveness of dye degradation, the impact of specific operational aspects was also carefully examined. These factors included the amount of catalyst, the length of exposure, the initial concentration of dye, and the pH levels.

CAPTER 2: LITERATURE REVIEW

2.1 Textile Dye Pollution

Textile dye pollution is a fairly recognized phenomenon leading to harmful water contamination impacts on the global level. 17-20% of the water pollution around the globe is the textile dyeing processes estimate. The country's rivers are majorly affected as often the water is not properly treated before being discharged into them. The pollutants affect the BOD, COD, TDS, TSS etc. affecting not only the quality of water but puts the aquatic life at risk. This further leads to damaging the whole ecosystem. The complexity and composition of textile Dye Pollution has been researched extensively and have mainly emphasized the condition of the research on the Health and Ecological Risks and Challenges in Wastewater Treatment.

Lara et al. provide a critical analysis of the recent practices on pretreatment innovations and sustainable dyeing techniques by doing a comprehensive intersection of textile dye wastewater and environmental sustainability [1]. They study the economic and technological feasibility fostering awareness where traditional methods lack and giving a solution for it.

Al-Tohamy et al. based on a very good comparison about the various physical and chemical methods used for dye removal which are effective but at the same time have come to an understanding of how none of the methods is economically viable for sufficiently treating such a big problem [2]. They compared physical and chemical methods to microbial approaches. Al-Tohamy et al. also reported combined approaches and recent technologies that can be promising for dye removal.

Substantial work has also been completed on synthetic dyes used in the textile industry by Hassaan et al., who examine a number of recent treatment techniques to manage textile wastewater, Toxicity of Azo Dyes, Health and Environmental Impacts of Dyes and

Advanced Oxidation Processes [3]. All of Current treatment methods are inadequate for complete removal of dye hence there is a high need of using AOPs to tackle dye pollution.

More recently, Tripathi et al. also looked at dye-polluted wastewater with an emphasis on eco-friendly technologies., i.e., Genetically Engineered Microorganisms (GEMs), Nanotechnology, Microbial Fuel Cells (MFCs), Microbial Biosorbents and Bioreactors [4]. Their study is useful in terms of merging Advanced biological, nanotechnology and engineered microbes to find effective treatment routes for contaminated textile wastewater.

Yaseen et al. continue to advance the field by looking at the characteristics of textile dye wastewater, the various treatment methods applied and the constituents of both real and synthetic effluents [5]. They rightfully note the influence of Dye Types and their complex aromatic structures. It offers a strong foundation for developing and evaluating new dye removal technologies, especially in photocatalysis and bioremediation studies.

2.2 Overview of Congo Red and Dye Pollution

Alhasan et al. used gum Arabic as a natural source for the green synthesis method for the degradation of CR dye [6]. The ZnO nanoparticles showed a calculated crystallite size of 42.7 nm. The optimum dye concentration of 20 mg L^{-1} gave rise to highest photodegradation results, and 4 mg mL^{-1} was the optimal photocatalyst loading with pH 8 used to achieve 99.5% degradation in 30 min of irradiation.

Using the bacterial strain Chryse bacterium geocarposphaerae DD3, Sarkar et al. checked the breakdown of Congo Red dye [7]. For 0.2 g/L of Congo Red, a photocatalytic efficiency of 96.52% was attained in 12 hours. For efficient wastewater treatment, the post-treatment toxicity decrease was thoroughly assessed.

Shaban et al. used Fe-chromite as a catalyst for degrading CR dye through the help of photocatalytic degradation in water and UV assisted-Fenton oxidation method too [8]. The photo-Fenton process surpassed and showed 100% degradation of Congo Red dye.

Kumar et al. used raw eggshell as catalyst for the breakdown of CR dye in the visible light region with using graphite carbon nitride [9]. They achieved catalyst removal around 90.5% under 90 min at 498 nm when subjected to visible light.

Mansour et al. studied the formation of hydroxyl radicals ·OH on how they degrade azo dye as congo red [10]. They applied Doehlert's experimental design to underline optimum conditions mainly initial Fe^{2+} concentration, current intensity, and contact time for the Congo red removal. The results showcased 81.1% removal rate of TOC after 300 mins of contact time.

Al-Farraj et al. use the Pechini sol–gel method to create $MgAl_2O_4$ nanoparticles [12]. The particles obtained were of spherical shape having an average diameter of 8.75nm. at pH of 3, optimal degradation occurred in a 50 mL Congo red dye sample with an initial concentration of 25 mg/L. occurred in 80 minutes, reaching 99.27%.

2.3 Green synthesis of ZnO photocatalyst

In 2022, Batra et al. [13] reviewed a comprehensive study on the environmentally friendly synthesis of ZnO-based nanoparticles and how they are used in the photocatalytic degradation of synthetic colours from wastewater [13]. In 2022, Tra et al. The synthesis pathways that use plant extracts, fungus, bacteria, and algae as a good alternative to conventional chemical methods. It looks into changes such heterojunction formation, hybrid composites, and doping. The dye degradation performance of various ZnO-based nanoplatforms is thoroughly compared, with particular attention to, synthetic dyes such as methylene blue, rhodamine B, and malachite green are commonly used as model

pollutants. The paper also highlights the importance of process factors like pH, light source, and catalyst dosage.

Devi et al. synthesized Undoped and Fe-doped ZnO nanoparticles (NPs) using leaf extract of Amaranthus spinosus as a reducing agent [14]. The analysis confirmed that the ZnO NPs possessed a rod-like morphology and a hexagonal wurtzite crystal structure. Upon Fe doping, a reduction in crystal size, solubility, and aggregation was observed. Among the synthesized NPs, under solar irradiance, 1 wt% Fe-doped ZnO prepared with *A. spinosus* extract achieved enhanced decolorization of indigo carmine dye, reaching 97% efficiency.

Boopathi et al. added to the conversation by using Psidium guajava (guava) leaf extract employed in the green synthesis of Fe-doped ZnO using plant-based extracts nanoparticles [15]. Strongly coupled solvers are more computationally intensive, but they are advantageous. Vaassen and Leonard demonstrated the advantages, as well as the computational challenges of strong coupling, in parametric space mostly associated with a higher degree of deformability of the structures/section, or when a larger portion of the structural response was included.

Sukri et al. reported the photocatalytic efficiency of zinc oxide nanoparticles by monitoring the degradation of dye that is Malachite Green under UV light exposure [16]. These ZnO-NPs were synthesized using a green approach, where Punica granatum (pomegranate) peel extract served as a natural stabilizing agent. A straightforward sol-gel method followed by calcination at varying temperatures (400°C, 500°C, 600°C, and 700°C) was employed to obtain high-purity ZnO-NPs with enhanced photocatalytic characteristics. Among the samples, the nanoparticles calcined at 700°C exhibited the highest efficiency, achieving approximately 99% dye removal within just 40 minutes.

Kaliraj et al. flower-shaped zinc oxide (ZnO/QNF) using extract of panos—a blend derived from four various Panax plants (Acanthopanax senticosus, Panax ginseng, Dendropanax morbifera and Kalopanax septemlobus,) [17]. The material was identified and measured using techniques like XRD, FTIR, XPS, and TEM. When tested under UV

light, the ZnO/QNF effectively removed industrial dyes—methylene blue, Eosin Y, and Malachite Green—achieving over 99% degradation of 15 mg/L dye solutions within 80, 90, and 110 minutes, respectively.

Stan et al. synthesized ZnO were successfully prepared by biological synthesis using aqueous extracts obtained from Allium sativum (garlic), Allium cepa (onion) and crispum (parsley) to study of dye with was highest due to garlic [18].

Nawaz et al. prepared ZnO by using ionic-liquid-based microwave-assisted extracts of Polygonum minus [19]. ZnO had a surface area of 353.11 m^2/g and a particle size of 32 nm. In a degradation time of 60 min, ZnO was able to eliminate 97.50% of the 40 mg/L MB.

Karthik et al. evaluated and compared different zinc oxide nanoparticles from Synadium grantii leaf extract with changing Cu-doping concentrations [20]. They used copper nitrate trihydrate and zinc nitrate hexahydrate as a starting material in extracts of the leaf part of the plant. The highest photocatalytic removal for MB, IC, and RhB dyes was of 3% and 5% Cu- doped samples.

Faisa et al. used aqueous fruit extracts of Myristica fragrans to bioaugmented zinc oxide nanoparticles (ZnO-NPs). The photocatalytic dye degradation was observed to be 88% of methylene blue dye in 140 min [21].

Using Coriandrum sativum leaf extract that was calcined at 100°C and 550°C, Yashni et al created ZnO NPs [22]. These particles had crystalline diameters of 60.85 and 55.13 nm, respectively, and band gaps of 3.56 and 3.72 eV. In contrast to those made at 100°C, the ZnO NPs generated at 550 °C exhibited superior structural characteristics.

Bhuyan proposed cheap, synthesis of (ZnO) using a green approach via 25% (w/v) of Azadirachta indica (Neem) leaf [23]. The biosynthesized were examined by (TEM), energy-dispersive X-ray spectroscopy (EDX), UV–visible spectroscopy (UV–vis), X-ray diffraction (XRD) and (FTIR). The ZnO obtained were of spherical shape, high purity and had a size around 9.6 to 25.5 nm.

2.4 Mechanism of Fe doped ZnO photocatalyst

Priyanka and Srivastava highlight the iron doped zinc oxide photocatalyst for wastewater infused with dyes by solution combustion synthesis method [24]. At ideal circumstances, a dye solution (acid red 1) with 50 mg/L initial concentration and 2730 Pt:Co units as initial color showed more than 71% removal rate of color, 94% dye was degraded, and 41% carbon removal took place.

Farahani et al. promisingly synthesized different doping percentages of Fe on ZnO for the degradation of Methylene Blue dye [25]. They achieved 98.84% removal rate at optimal conditions and studied the photocatalyst regeneration as well.

Wu et al. experimentally demonstrated 1% Fe doped ZnO to give 2.2 times greater Methylene Blue dye degradation over pure ZnO in the presence of simulate solar light and that's how the activity of photoreduction was observed [26]. They use of electrospun technology was done in this study.

Dharmana et al. described the characteristics of Fe doped ZnO gave rise to a large surface area [27]. They were created via hydrothermal synthesis process and observed how it increases the photocatalytic efficiency under the presence of light. They used zinc acetate dihydrate as a precursor. Thus, during 120 min the degradation was 95.8% more of Methylene Blue dye.

Habba et al. used Iron (1%) as a doping material instead of Co, Cr, Ag, Sn etc. because it a lowest degradation impact on the environment [28]. The shape of the iron doped nanoparticles was found to be nanowires like. Another observation was that the bandgap decreased from 3.29 eV (ZnO) to 3.25 eV (Fe:ZnO). There occurred a 9%, 20%, and 5% hike in the photo-degradation rate of the MB, MO, and AR14 respectively.

Ong et al. gave importance to adsorption merged with photocatalysis occurring due to solar and how it improved the degradation of carcinogenic Congo Red dye using Fe doped ZnO [29]. The characterization techniques proved that doping Fe with ZnO improved photocatalytic efficiency. The performance of nanofiltration (NF) in terms of removing CR residues from water and their fouling behavior after photocatalysts have been separated was examined.

Popa et al. showcased a 96% degradation efficiency of Rhodamine B dye when multi walled nanotubes tied up with Fe doped ZnO in varying with weight ratios of 1:3, 1:5 and 1:10 and thereafter photoluminescence (PL) and photocatalytic properties were studied [30].

Xiao et al. examined the stability of both ideal polar and non-polar surfaces when ZnO nanoparticles are doped with Fe [31]. Only on polar surfaces, where the dipole moments are severely suppressed, can Fe dopants stabilize the system. The key observation was that the total dipole moment of ZnO NPs is suppressed by Fe dopants-assisted charge transfer, and the Fe^{3+} cations saturate dangling bonds stabilizes the ZnO NPs.

Chai et al. employed Hibiscus rosa-sinensis leaf extracts to create magnetic iron-doped ZnO nanoparticles (Fe-ZnO) using green synthesis [32]. Results from Fourier-transform infrared spectroscopy verified that leaf extracts included phytochemicals that influenced the development of nanoparticles. The average particle sizes were between 15 and 170 nm which was confirmed via FESEM. In comparison to pure ZnO and commercial ZnO, they examined the stability of Fe-ZnO to exhibited outstanding photocatalytic, antibacterial, and antifungal properties.

Using plant leaf extract from the Mangifera indica plant as a natural reducing agent, Jadon et al. incorporated an environmentally friendly process for creating ferric oxide nanoparticles (Fe_2O_3), zinc oxide nanoparticles (ZnO), and Fe_2O_3/ZnO nanocomposite was reported with an average diameter of 11.33 nm, 14.31 nm and 9.80 nm [33]. They looked into the stability of the Fe_2O_3/ZnO nanocomposite's light-driven catalytic efficiency, which at an optimal catalyst dose degrades methyl orange dye by around 91.07% in 150 minutes.

Jha and Chakraborty obtained NPs using $FeSO_4.7H_2O$ as a starting agent and Shorea robusta (sal) leaf extract as reductant under optimum condition of 1 mM concentration of precursor and a ratio of 1:1 $FeSO_4.7H_2O$ to Sal leaf extract [34]. The nanoparticles of size 54-80 nm were formed having a spherical shape which was analyzed by TEM and AFM images. The photocatalytic efficiency was found to degrade 96% Congo Red.

Together, these papers form the basis of current best practice in green synthesis of zinc oxide.

CHAPTER 3: MATERIALS AND EXPERIMENTAL METHODS

3.1 Introduction

This section showcases all the materials and reagents required throughout the experimental work and the specified chemicals used during the synthesis and doping processes. The details about the purity, nature and source of each chemical used has been mentioned. Plus, the step-by-step experimental process on preparation of extract, reaction conditions, doping concentrations and post-synthesis treatments such as drying, calcination, and storage is elaborated. The workflow of the experimentation has been arranged from initial synthesis to final product formation.

3.2 Materials

Table 3.1 - List of the chemical reagents used for the experimental work

Reagent	Molecular formula	Company
Congo Red	$C_{32}H_{22}N_6Na_2O_6S_2$	Merck
Iron Nitrate Nonahydrate (>98%)	$Fe\ (NO_3)_3.9H_2O$	Merck
Sodium hydroxide pellets (>97)	NaOH	Merck
Zinc acetate dihydrate (>98%)	$(CH_3COO)_2\ Zn.2H_2O$	Merck

**The reagents utilized for the study were used as it is without additional purification.*

3.3 Experimental Methods

3.3.1 Preparation of plant Extract

In a 500 mL glass beaker, we mixed 50 g of Coriandrum sativum leaves with 200 mL (w/v) of deionized water to prepare the plant extract [18]. We stirred this mixture using a magnetic stirrer and heated it to 60 °C for 30 minutes, or until the water turned dark yellow [9], [18]. After the solution cooled down to room temperature (25 °C ± 2 °C), we filtered it through Whatman filter paper (No. 40). The filtered liquid was gathered in a clean glass bottle and stored at 4 °C [9], [18].

3.3.2 Green Synthesis of Fe-Doped ZnO Nanoparticles

The Iron doped zinc oxide nanoparticles were created using a green method with leaf extract derived from Coriandrum sativum (commonly known as coriander). It started by mixing 0.22 grams of zinc acetate dihydrate (Zn $(CH_3COO)_2 \cdot 2H_2O$) and 0.00810 grams of ferric nitrate nonahydrate (Fe $(NO3)_3 \cdot 9H_2O$) in 50 mL of distilled water. This amount of ferric nitrate led to a 2% iron (Fe) doping concentration by weight. Magnetic stirring was performed at a speed of 200 revolutions per minute (rpm) for 10 minutes to dissolve everything.

Then, 1 mL of coriander leaf extract was mixed that served as functioning as both a reductant and a capping agent during the making [9]. The pH of the solution was then raised to 12 by dropping 2.0 M sodium hydroxide (NaOH) slowly, which resulted in the appearance of pale white precipitate indicative of ZnO nanoparticle formation [11], [17], [18]. In order to provide uniform nucleation and controlled growth of the nanoparticles, the mixture was again stirred at 1000 rpm for a further 20 minutes [17], [18].

Fig. 3.1 - Experimentation Setup

Finally, the centrifuged precipitated nanoparticles were centrifugation at 4000 rpm for 25 minutes. It was afterwards washed well with distilled water and ethanol in order to remove any other remaining impurities present and thus the resulting powder was dried in a hot air oven at 100°C overnight and calcinated at 500°C, producing the desired Fe-doped ZnO nanoparticles.

Fig. 3.2 - Fe doped ZnO nanoparticles

3.4 Photocatalytic activity of Congo Red dye degradation

The primary objective of this experiment was to determine how effectively our Fe-doped ZnO nanoparticles degraded Congo Red dye upon exposure to natural sunlight. We conducted a batch experiment, introducing a set amount of the Fe:ZnO nanoparticles into 500 mL of a solution of Congo Red (at a certain concentration). We began by very quickly stirring this mixture for thirty minutes in the dark. In this way, we could be sure that any later dye degradation that we observed was the result of only the photocatalytic action of the nanoparticles in the light. To further use for UV-Visible spectrophotometer a 3 mL sample was taken out at uniform intervals of time and was centrifuged at 4000 rpm to isolate the nanoparticles from the liquid. The resulting clear liquid was then scanned on a UV-Visible spectrophotometer, which measures light absorption at 498 nm, the wavelength at which Congo Red absorbs least light. Finally, we used the standard formula to determine the percentage of Congo Red that was degraded by dividing the initial amount of dye present by the amount still present which is given by:

$$\%\, Degradation = \left(1 - \frac{Ct}{C0}\right) \times 100 \tag{3.1}$$

where, C_0 = initial (t =0),

C_t = final concentration (t = t)

3.5 Characterization

The physicochemical characteristics were analyzed to know the composition, structure and optical behavior of the synthesized nanoparticles. X-ray diffractometer was performed using a Rigaku Miniflex 600 to identify the crystalline structure. Fourier Transform Infrared (FTIR) spectroscopy, conducted using a Shimadzu IR Affinity spectrophotometer, was used to identify the involved Carbon bonds and functional groups in the nanoparticles. UV-visible spectra were performed on several samples to study the optical absorption behavior. A Carl Zeiss field emission SEM, equipped with an EDS system, was employed to examine the surface structure and compositions of the photocatalyst. The combined analysis from these techniques provided comprehensive insights into the physicochemical properties of Fe-doped ZnO.

CHAPTER 4: RESULTS AND DISCUSSIONS

4.1 Characterization of ZnO and Iron doped ZnO nanoparticles

4.3.1 XRD diffraction analysis

X-ray diffraction (XRD) analysis was carried out to know the crystalline phase purity, structure and size of crystallites in the nanoparticles synthesized using Debye–Scherrer formula:

$$D = \frac{K\lambda}{\beta cos\theta} \quad \text{..... (4.1)}$$

Here,

D = avg crystallite size in mm

K = shape factor

λ = wavelength set at 0.15406 nm

β = full width

θ= Bragg's diffraction angle in radian units

For Pure ZnO Nanoparticles:

Pure ZnO XRD pattern (Figure4.1) reflects sharp and clear peaks, demonstrating a high level of crystallinity. The characteristic diffraction peaks are found at the following 2θ values: 31.73°, 34.39°, 36.21°, 47.48°, 56.54°, 62.84°, 66.37°, 67.91°, and 69.08°. The planes are referring to the structure of ZnO who's structure is hexagonal wurtzite, and the pattern closely matches. The created Zinc Oxide nanoparticles indicate no other or impurity peaks ensures the phase purity.

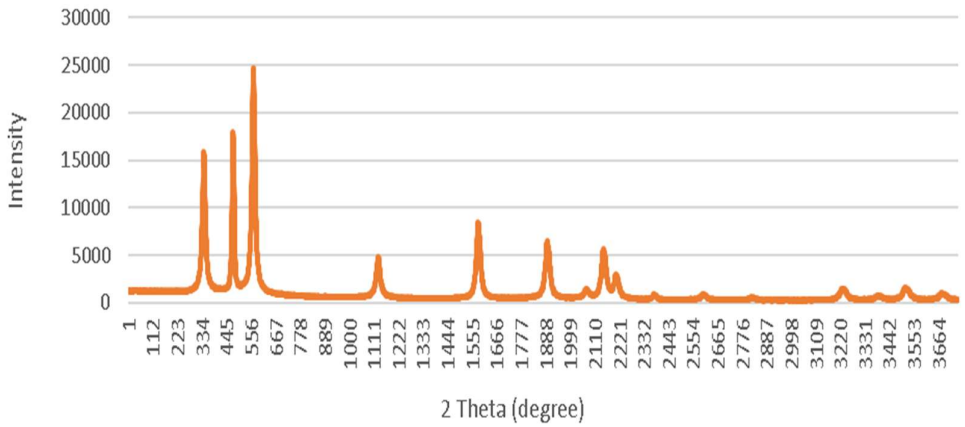

Fig. 4.1 - XRD analysis of Pure ZnO

Zinc Oxide nanoparticle with Fe doping:

The XRD pattern of ZnO doped with Iron (Figure 4.2) shows the same diffraction pattern as pure ZnO, which verifies that Fe doping does not affect the underlying hexagonal wurtzite structure. However, minor shifts in the positions of the peaks as well as intensity changes are observed, indicating successful Fe^{3+} ions' substitution for Zn^{2+} sites in the ZnO lattice. Uniquely prominent diffraction peaks are again evidenced at approximately: 31.72°, 34.36°, 36.11°, 47.41°, 56.45°, 62.75°. The respective crystal planes are same as above of pure ZnO, indicating that the crystal structure is preserved. The lattice distortion and shrinkage are the reason for slight shift to increased 2θ values may be attributed to the smaller ionic size of Fe^{3+} (0.64 Å) compared to Zn^{2+} (0.74 Å). The doping of Fe into ZnO lattice is impurity free as there are no peaks of detected vibrational modes validate the incorporation of Fe within the ZnO lattice.

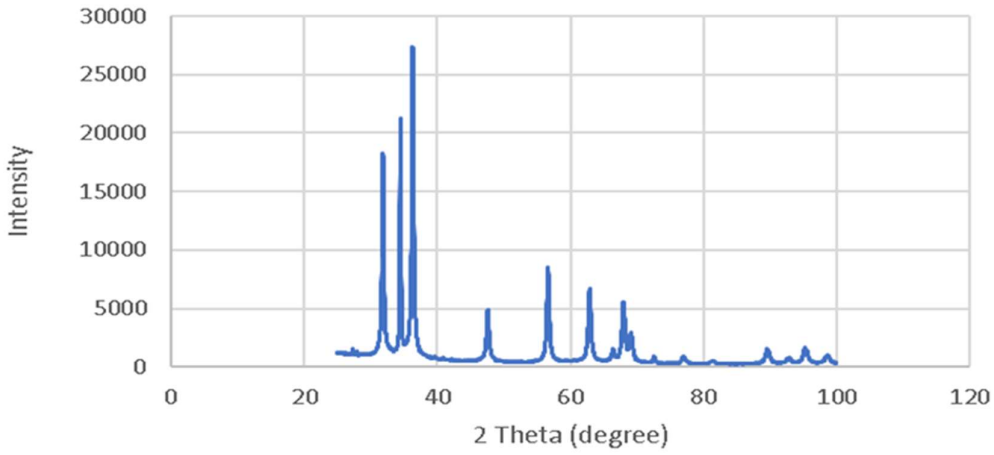

Fig. 4.2 - XRD analysis of Fe doped ZnO

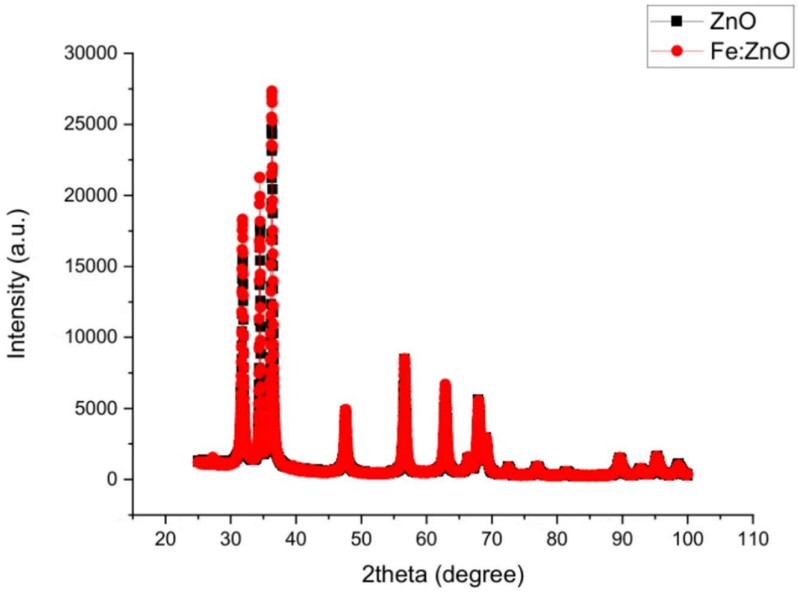

Fig. 4.3 - XRD spectrum of Iron doped and Pure ZnO

The calculated crystal size of pure ZnO was 22.8 nm while that of Iron doped ZnO was 29.5 nm which suggests the growth behavior of the nanoparticles.

4.3.2 Fourier Transform Infrared Analysis

FTIR spectroscopy was utilized to examine the vibrational bonds and identify the functional moieties existing in the Fe-doped ZnO nanoparticles. The FTIR spectrum is measured in the wavenumber region of 4000 cm^{-1} to 400 cm^{-1}, as indicated in Figure 4.4.

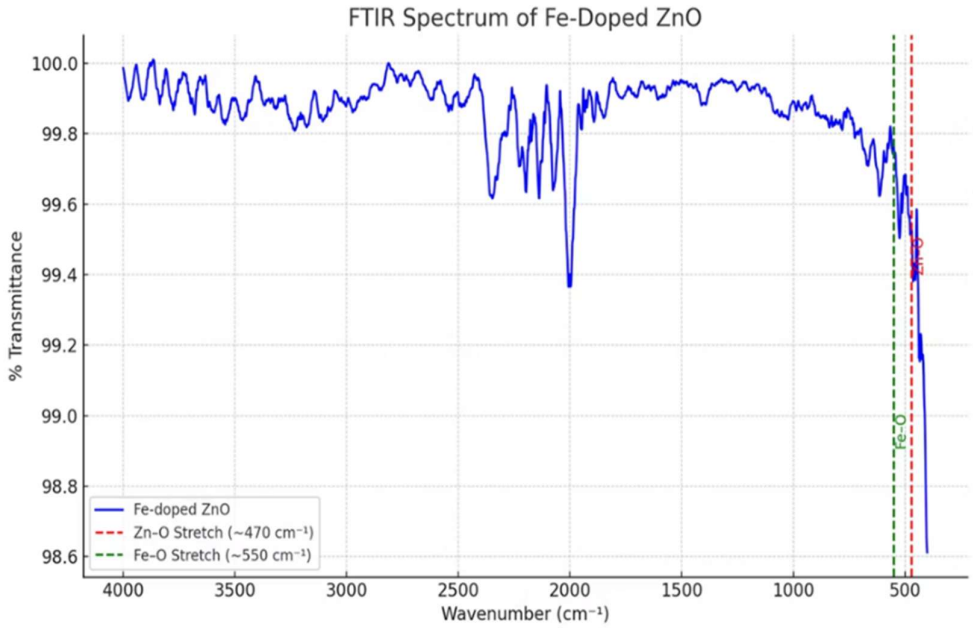

Fig. 4.4 - FTIR analysis of Fe doped ZnO

The key observations are:

Broad Range (4000–1500 cm^{-1}): It is observed in this range that there are minor changes in transmittance but no prominent absorption peaks. This reflects the absence of significant organic groups which are reactive such as –OH, C=O, or C–H. It can be inferred that all such phytochemicals incorporated during synthesis are either decomposed or removed during the drying and calcination process.

Sharp Absorption Near 470 cm^{-1}: There is a clear peak at ~470 cm^{-1} for the Zn–O stretching vibration, indicative of ZnO nanoparticle formation. These values are consistent with reported literature values for metal-oxygen stretching mode in ZnO lattices. The existence of both Zn–O and Fe–O vibrational modes establishes that the Fe^{3+} ions have been doped into the ZnO crystal lattice as replacements for Zn^{2+} without creating distinct Fe-based phases.

Peak Near 550 cm^{-1}: There is a weaker but distinct peak near ~550 cm^{-1} due to the Fe–O stretch, those detected vibrational modes validate the incorporation of Fe within the ZnO lattice. lattice.

The peak corresponds to characteristic vibrations of Fe–O linkages in the structure. bonds in Fe-doped oxide material. Lack of other peaks corresponding to organic compounds (such as C=O or –OH) verifies that the phytochemicals of coriander leaf extract were successfully eliminated or broken down, and trace stabilizing agents may be left behind.

4.3.3 FESEM and EDS analysis

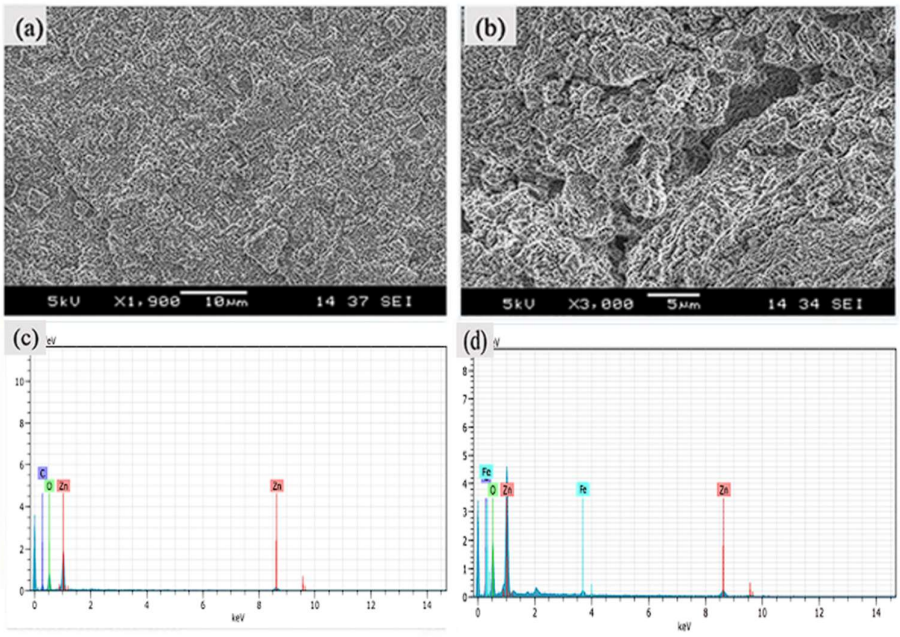

Fig. 4.5 - FESEM analysis Pure ZnO and Iron doped ZnO

Morphological investigation (surface texture) of doped (Fe:ZnO) and pure Zinc oxide nanoparticles. The SEM images (Figure 4.5 a, b) clearly indicate that they were composed of nano-sized particles, which are agglomerated into larger powder particles. Fe:ZnO exhibited clustered and smaller nanoparticles. This is a clear indication that introducing Fe into the ZnO structure resulted in a more homogeneous mixture, reducing the extent of

agglomeration. The EDS spectra (Figure 4.5 c, d) indicate zinc (Zn), iron (Fe), & oxygen (O) present in synthesized Fe-doped ZnO nanoparticles. The clearly identifiable iron peaks confirm that the doping of Iron into the ZnO lattice was successful. The atomic percentages of Zn, Fe & O were determined to be 14.82%, 1.18%, and 49.55%, respectively.

4.2 Photocatalytic activity

The operational factors such contact time, photocatalyst loading, concentration of dye, and pH of the dye solution were used to examine produced photocatalysts' photocatalytic dye degradation capability. It was also noticed which elements affected the degrading efficiency.

4.2.1 Effect of Contact Time

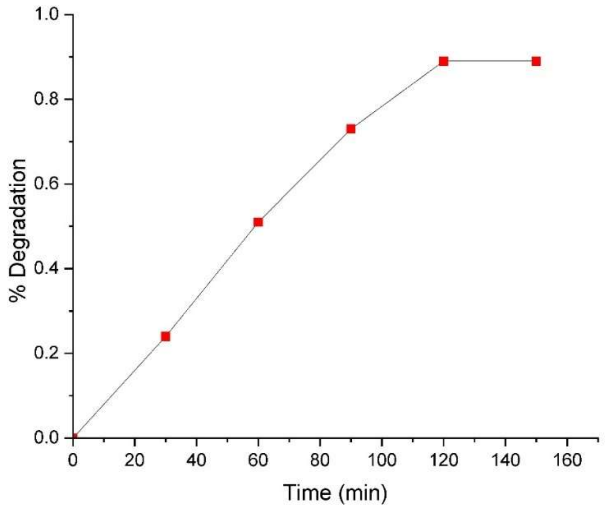

Fig. 4.6 - Illustrates the influence of irradiation time on the degradation efficiency of Congo Red-dye using Fe-doped ZnO nanoparticles. The experiment was conducted with a photocatalyst dose of 200 mg, an initial dye concentration of 30 ppm, and solution pH of 7.

A control experiment was carried out with Congo Red dye solute dispersed in water under sunlight without a photocatalyst, and it was observed that the dye concentration does not reduce after 120 min. It means that the photolysis of Congo Red molecules

is practically negligible [27].

Figure 4.6 shows the effect of irradiation time (between 0 and 150 minutes) on Congo Red dye degradation. In a standard photocatalytic test, 100 mL of 30 ppm Congo Red dye (adjusted pH of 7) was exposed to 200 mg of Fe:ZnO photocatalyst. The results indicated that Congo Red dye was degraded better with longer irradiation times. However, after 120 minutes of degradation, steady-state degradation or no degradation was observed. Therefore, 120-minutes was determined to be the optimal contact time.

4.2.2 Effect of Catalyst Dosage

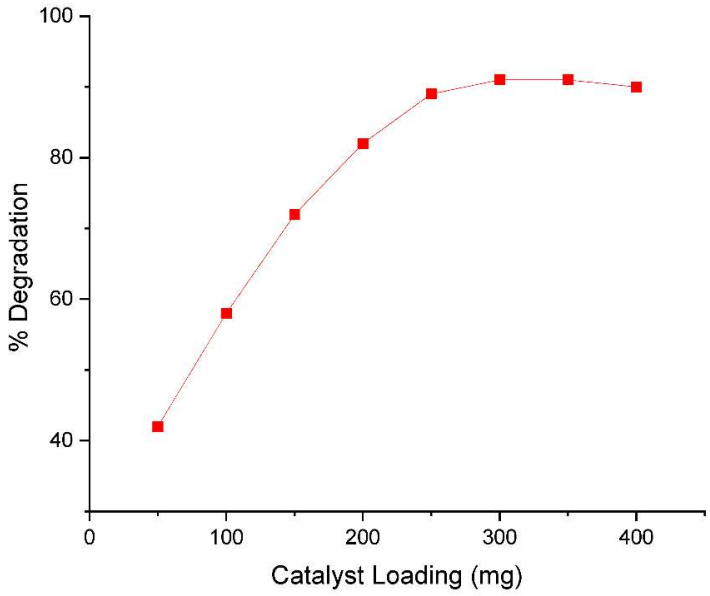

Fig. 4.7 - Shows the impact of varying catalyst dosages on the degradation of Congo Red dye using Fe-doped ZnO nanoparticles. The study was carried out with a dye concentration of 30 ppm, a contact time of 120 minutes, and a pH of 7.

Fig 4.7 shows the effect of catalyst loading (50 mg to 400 mg) on Congo Red dye degradation with Fe:ZnO nanoparticles. Under the experiment (100 mL of 30 ppm of Congo Red dye at pH 7), dye degradation significantly increased from 43.25% to 88.06% when the catalyst is raised from 50 mg to 400 mg for 120 minutes. This is because there are increased active surface sites available [26]. But an increase in the catalyst to 400 mg

caused a modest decline in efficiency due to catalyst overloading that resulted in particle agglomeration and lowering of light penetration. Hence, 300 mg was discovered as the best catalyst loading for maximum degradation of dye.

4.2.3 Effect of Dye Concentrate

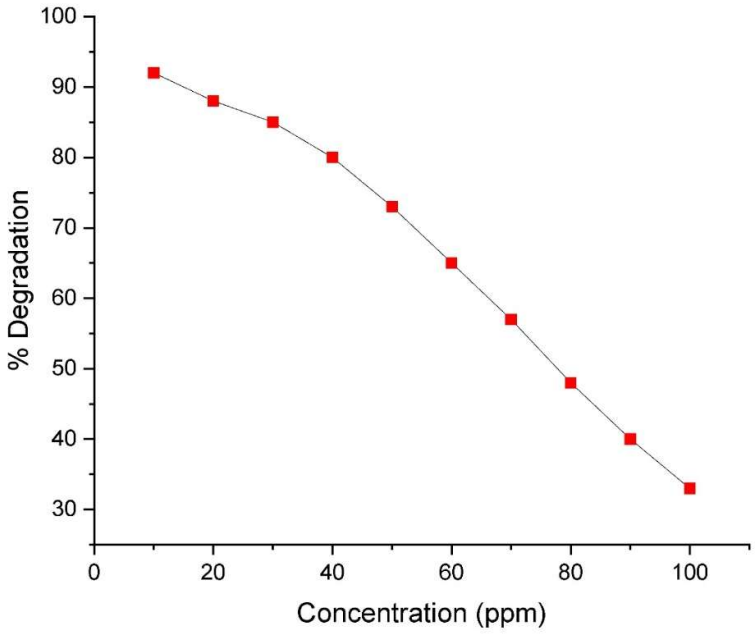

Fig. 4.8 - Illustrates how varying the initial concentration of Congo Red dye affects its degradation using Fe: ZnO nanoparticles. The experiment was conducted under controlled conditions with a 300 mg catalyst dosage, 120 minutes of irradiation, and a neutral pH of 7.

The rate of Congo Red dye degradation is shown to be 91.50% with a 10ppm dye concentration, while it drops to 33.37% with a dye concentration of 100 ppm.

This effect could result from an elevated dye concentration, the saturation of molecules of dye on the catalyst interface results from adsorption with remaining active sites available for the photodegradation to take place. Also, with increasing dye concentration the number of arriving incident photons who are meant to reach the photocatalyst surface reduces hence activation reduces. As a result, the photocatalysts' excitation is lowered, thus impacting the photodegradation efficiency overall [27][28].

4.2.4 Effect of pH

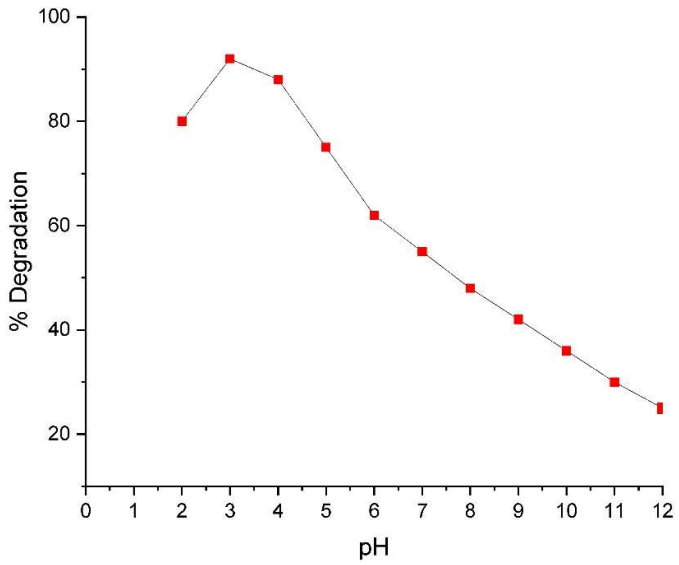

Fig. 4.9 - Illustrates the impact of solution pH on the degradation efficiency of Congo Red dye utilizing Fe:ZnO nanoparticles. The study was carried out with a contact time of 120 minutes, a catalyst amount of 300 mg, and an initial dye concentration of 10 ppm.

Figure 4.9 determines how to optimize the efficiency while minimizing any negative consequences. It demonstrates maximum degradation at pH 3, exhibiting excellent light-driven catalytic efficiency in acidic conditions. The acidic reaction environment enhances Fe:ZnO activity by increasing the protonation, and thus the affinity of the negatively charged dyes through electrostatic interaction.

The efficiency of degradation decreases with increasing pH due to the following reasons:

- Lessened surface charge interaction at increased pH.
- Possible dye molecule repulsion due to a negatively charged catalyst surface.
- Hydroxyl radical (•OH) production becomes increasingly unfavourable at higher pH values.
- Photocatalytic performance is pH-sensitive, requiring optimization for maximum

efficiency.

The charge of a catalyst's surface can be altered based on its pH value at which the surface of the material carries a neutral charge in basic electrolytic conditions, the active surface of the photocatalyst is positively charged in acidic solutions and negative in basic solutions. The maximum adsorption of CR dye was noticed at a pH of 3 (acidic).

In contrast, in a basic solution, both the dye and the catalyst surface are negatively charged. This results in repulsive forces that obstruct the Congo Red degradation, thus leading to lower efficiency.

4.2.5 Doping influence at optimal conditions

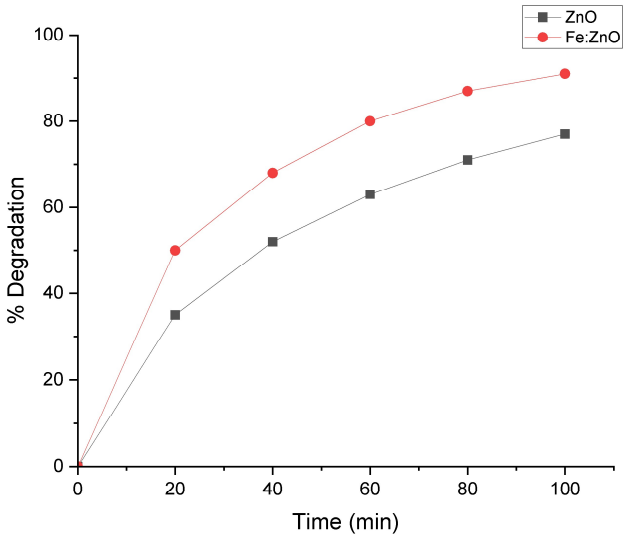

Fig. 4.10 - Demonstrates how different Fe doping levels influence the degradation of Congo Red dye using Fe: ZnO nanoparticles. The experiment was performed with a photocatalyst dosage of 300 mg, initial dye concentration of 10 ppm, pH 3, and an irradiation period of 120 minutes.

This investigation assessed the photocatalytic efficacy of Fe:ZnO nanocomposites against pure ZnO under optimized conditions (catalyst dosage 300 mg, initial Congo Red dye concentration 10 ppm and solution pH 3). As shown in Figure 4.10, the Fe:ZnO nanocomposite showed significantly better degradation performance (91% efficiency)

while that of pure ZnO (69.30%). The superior light-driven catalytic efficiency of Fe:ZnO is due to its higher charge carrier separation ability that efficiently reduces the photo generated recombination strategy, thus increasing its degradation efficiency [29].

4.3 Kinetic study on photocatalytic degradation

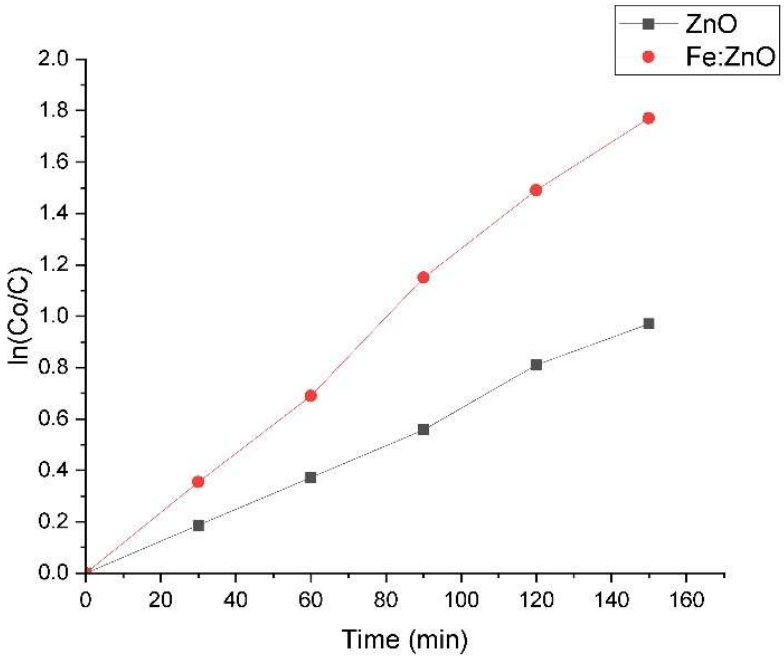

Fig. 4.11 - Depicts the pseudo-first-order kinetic plot for the degradation of Congo Red dye facilitated by Fe:ZnO nanoparticles.

According to the results, the kinetics of Congo Red dye breakdown by synthesized ZnO and Fe: ZnO photocatalysts was studied under optimal operating conditions (300 mg/100 mL catalyst, pH=5, 10 ppm dye). Figure 4.11 shows the resulting fitting correlation coefficient (R2), which was an extremely good match between experimental results and model [30]. The rate constant of pure ZnO was expected to be lower than Fe:ZnO, as Fe:ZnO's photocatalytic efficiency was enhanced.

The dynamics of compound degradation obeyed pseudo-first order reaction kinetics, and the value of k was calculated from the equation:

$$ln\frac{C0}{Ct} = kt \tag{4.2}$$

Here, C_0 = initial dye concentration

C_t = final concentration after t minutes of irradiation.

k = rate constant

Figure 4.11 shows the resulting fitting correlation coefficient (R^2), which was an extremely good match between experimental results and model. The rate constant for undoped ZnO was anticipated to be lower compared to Fe-doped ZnO, due to the improved photocatalytic performance exhibited by the latter.

4.4 Mechanism of dye degradation

The dye degradation process degrades the dye through four steps as given below:

1. Photocatalytic Activation and Charge Separation: When the Fe:ZnO photocatalyst is exposed to sunlight, it becomes photoactive, and begins the formation of electron-hole pairs. In this typical process, electrons of the lower energy band (VB) absorb sunlight and are excited to the higher energy band (CB) producing positively charged holes in the lower energy band. the light-driven catalytic efficiency is triggered due to this charge separation, starting the reaction.
2. Improvement by Iron (Fe) Doping: The addition of iron (Fe) incorporated into the ZnO lattice plays a crucial part in enhancing the photocatalyst's efficiency. Iron helps reduce the rapid recombination of electrons and holes, a process that typically limits photocatalytic performance. This significant improvement is largely attributed to the Fe^{3+}/Fe^{2+} redox cycle, which promotes effective charge separation and facilitates electron transfer, ultimately resulting in higher overall degradation efficiency.
3. Reactive Oxygen Species (ROS) Formation: Throughout the entire process of the reaction, Fe^{3+} ions act as electron acceptors by capturing captured photoexcited electrons and causing Fe^{3+} ions to get reduced to Fe^{2+} ions. The Fe^{2+} ions further react with molecular oxygen (O_2) and this creates superoxide radicals ($O_2^{\bullet -}$), which are extremely reactive and play a major role in degrading pollutants.
4. CR dye removal via Photocatalysis: In the last step, the generated hydroxyl radicals (•OH) formed in the course of the reaction are engaged in the disintegration of the CR dye molecules. The highly reactive species degrade the structure of the dye. Therefore,

the production of •OH radicals is the main motive for the effective breakdown of Congo Red, which is significantly boosted by the improved charge separation and enhanced generation of reactive species made possible through Fe doping in the ZnO photocatalyst.

4.5 Conclusion

In this study, environmentally sustainable method for nanoparticle synthesis was applied to successfully create ZnO and Iron-doped ZnO (Fe:ZnO) nanoparticles. Their physical structure, morphological features, and optical attributes studied by X-Ray Diffraction, FTIR, FESEM, EDS, & UV-Visible spectroscopy. Upon validation of their physicochemical characteristics, these NPAs were employed as effective photocatalysts for assessing the breakdown of an organic CR dye in the influence of natural sunlight irradiation. We further systematically optimized a few essential operation factors such as irradiation time, effect of catalyst dose, pH and dye concentration and pH to obtain their ideal photocatalytic efficiency. Under optimal conditions (300 mg catalyst dosage, 10 ppm initial Congo Red and pH 3), the Fe:ZnO photocatalyst reached a maximum degradation efficiency of 91%. Fe-doped ZnO had better photocatalytic property as compared to pure ZnO. This improved performance has been largely credited to its narrowed energy gap with VB and CB and the effective suppression of recombination of electron-hole pair, resulting in overall enhanced photocatalytic efficiency.

CHAPTER 5: SUMMARY, KEY CONCLUSIONS, AND RECOMMENDATIONS FOR FUTURE WORK

5.1 Summary of Work

In this study, the main focus was to understand how ZnO can be synthesized by utilizing Coriandrum sativum (coriander) extract derived from leaves which reduces another compound as well as act as a capping tool and subsequently doping the photocatalyst with Fe to improve its photocatalytic degradation for Congo Red dye. To precisely investigate the optimizing parameters constituting the factors influencing the Efficiency of degradation. The sustainable, green synthesis route is cost-effective and easy and is very efficient in producing this material. By incorporating iron (Fe) as a dopant into ZnO, the present study aimed to enhance the photocatalytic efficiency for degrading harmful dyes in wastewater. Their physical structure, morphological features, and optical attributes investigated through X-Ray Diffraction, FTIR, FESEM, EDS & UV-Visible spectroscopy. These methods included X-ray diffraction (XRD) to determine crystal structures, FTIR for functional group identification, FESEM and EDS for surface morphology and elemental composition analysis, and UV–Visible spectroscopy for optical properties analysis. These descriptions confirmed the successful formation of Fe: ZnO nanoparticles with potential characteristics for photocatalytic applications. To calculate the photocatalytic performance of these nanoparticles, the breaking down of CR dye under natural sunlight irradiation was monitored. The study examined the influence of factors like pH, catalyst dosage, concentration of dye & irradiation time on the degradation path. Under these conditions, the best outcome was achieved that degradation of dye was around 91% by using 300 mg of catalyst with dye concentration of 10 ppm and pH 3. Most important to our photocatalytic pursuits was the discovery that adding Fe to ZnO resulted in decreased electron-hole recombination, a malignant trait of many photocatalysts. This modification played important role in generating a larger amount of oxidative radical intermediates (ROS) including hydroxyl radical (•OH), that is solely responsible for the dye molecule degradation process. In conclusion, the current study demonstrated that green-synthesized Fe:ZnO NPs offer a durable, cheap, and sustainable solution for the decolorizing of dye-polluted wastewater, and thus have great promises for real life applications in environmental remediation technologies.

5.2 Key Conclusions

- XRD analysis: The calculated crystallite dimension of pure ZnO was found to be 22.8 nm while that of ZnO doped with iron was found to be 29.5 nm
- Doping ZnO with Fe: The 2%, iron (Fe) by weight was doped and the size of the nanoparticle increased due to the presence of greater density of surface-active sites suggesting the growth behavior of the nanoparticles.
- % Degradation: Traditional analytical solutions overpredict the % degradation to 99.5% which is in accordance with the literature. The value I got was around 91%
- Factor affecting photocatalytic degradation: The role of pH, time catalyst loading and dye concentration in modulating dye degradation, aiming to identify optimal conditions for maximum pollutant removal.

5.3 Limitations of Study

- Restricted Light Environment (Natural Sunlight without Tint or Reflections) The light-driven catalytic efficiency was tested with only natural sunlight. Since the intensity of sunlight that hits a material can vary greatly due to weather, time of day, and location it would be hard to ensure reproducibility of results. The performance under controlled artificial light sources, such as UV or visible lamps, was not investigated.
- Concentrating on One Dye (Congo Red) In their degradation experiments only one model dye, Congo Red, was used. The pilot study fails to measure the photocatalyst's performance against a wider diversity of dyes or actual textile effluents that frequently have mixed contaminants.

5.4 Future Perspectives

- Use on Actual Industrial Wastewater: In future work, it would be valuable to test the photocatalyst's effectiveness on actual industrial wastewater samples, rather than just synthetic dye solutions. Of course, real textile effluents are much more complicated, usually including a cocktail of different dyes, salts, surfactants, and sometimes heavy metals.
- Expanding the Field to Other Colorants Broadening the Scope to Other Dyes

- A primary goal of this study was to generically explore the conditions where surfactants are useful, so we used Congo Red as the model pollutant. However, a broader range of widely used dyes like Methylene Blue, Methyl Orange, and Rhodamine B are missed to widen insight across various dyes.
- Regeneration and Reusability of the Catalyst: The usefulness of any photocatalyst is checked by its ability to maintain its activity over multiple cycles of use. Thus, Future research should explore the stability, regeneration, and reusability of Fe:ZnO nanoparticles after multiple degradation cycles and observe the material's long-term performance, efficiency and cost-effectiveness on industrial applications.
- Development of Composite Photocatalysts: Combining Fe:ZnO with supporting materials like activated carbon, biochar, or clay as these materials are characterized by their high surface area and high adsorption capacity could increase the overall photocatalytic performance, structural performance and larger degree of reusability as well.

REFERENCES

1. L. R. Lara, I. Cabral, and J. Cunha, “Ecological approaches to textile dyeing: A review,” *Sustainability*, vol. 14, no. 14, art. 8353, 2022, doi: 10.3390/su14148353.
2. R. Al-Tohamy, S. S. Ali, F. Li, K. M. Okasha, Y. A.-G. Mahmoud, T. Elsamahy, H. Jiao, Y. Fu, and J. Sun “A critical review on the treatment of dye containing wastewater: Ecotoxicological and health concerns of textile dyes and possible remediation approaches,” *Ecotoxicol. Environ. Saf.*, vol. 231, art. 113160, 2022, doi: 10.1016/j.ecoenv.2021.113160.
3. M. A. Hassaan and A. El Nemr, “Health and environmental impacts of dyes: Mini review,” *Am. J. Environ. Sci. Eng.*, vol. 1, no. 3, pp. 64–67, 2017, doi: 10.11648/J.ENV.20170103.13.
4. M. Tripathi, S. K. Patel, M. R. Khan, D. K. Saini, S. S. Singh, and P. Singh, *“Recent strategies for the remediation of textile dyes from wastewater: A systematic review,”* Toxics, vol. 11, art. 940, 2023, doi: 10.3390/toxics11110940.
5. D. A. Yaseen and M. Scholz, “Textile dye wastewater characteristics and constituents of synthetic effluents: A critical review,” *Int. J. Environ. Sci. Technol.*, vol. 16, no. 2, pp. 1193–1226, 2019, doi: 10.1007/s13762-018-2130-z.
6. H. S. Alhasan, R. A. Khater, S. A. Alqarni, A. S. Alnoman, S. S. Alqahtani, A. B. Alzahrani, and M. A. Al-Ghamdi, *“Toxic Congo Red dye photodegradation employing green synthesis of ZnO nanoparticles using gum arabic,”* Water, vol. 16, no. 15, p. 2202, 2024, doi: 10.3390/w16152202.
7. S. Sarkar, R. Paul, A. Ghosh, and T. K. Dutta, *“Decolourisation and biodegradation of textile diazo dye Congo Red by Chryseobacterium geocarposphaerae DD3,”* Sustainability, vol. 13, no. 19, art. 10850, 2021, doi: 10.3390/su131910850.
8. M. Shaban, M. M. El-Hag Ali, A. M. Abukhadra, and A. A. El-Salam, *“Photocatalytic degradation and photo-Fenton oxidation of Congo Red dye pollutants in water using natural chromite—Response surface optimization,”* Appl. Water Sci., vol. 7, pp. 4743–4756, 2017, doi: 10.1007/s13201-017-0637-y.
9. J. Ambigadevi and P. S. Kumar, “Enhanced photocatalytic removal of Congo Red dye using eggshells infused with graphitic carbon nitride composites,” *Int. J. Chem. Eng.*, art. 5541488, 2025, doi: 10.1155/ijce/5541488.
10. D. Mansour, M. F. El-Shazly, A. A. Radwan, H. A. Khedr, M. R. El-Aassar, and A.

M. Atta, *"Removal of Congo Red dye by electrochemical advanced oxidation process,"* Sustainable Water Resour. Manag., vol. 10, no. 41, pp. 1–15, 2024, doi: 10.1007/s40899-023-01022-x.

11. Wikipedia contributors, "Industrial dye degradation," *Wikipedia*, 2023. [Online]. Available: https://en.wikipedia.org/wiki/Industrial_dye_degradation
12. E. S. Al-Farraj and E. A. Abdelrahman, "Efficient photocatalytic degradation of Congo Red dye using $MgAl_2O_4$ nanoparticles," *ACS Omega*, vol. 9, no. 1, pp. 1–12, 2024, doi: 10.1021/acsomega.3c08485.
13. V. Batra, I. Kaur, D. Pathania, S. Sonu, and V. Chaudhary, *"Efficient dye degradation using green synthesized ZnO-based nanoplatforms: A review,"* Appl. Surf. Sci. Adv., vol. 11, art. 100314, 2022, doi: 10.1016/j.apsadv.2022.100314.
14. S. Aiswarya Devi, B. Prasanna, and G. R. Kumar, *"Undoped and Fe-doped ZnO nanoparticles using Amaranthus spinosus leaf extract,"* J. Water Process Eng., vol. 49, p. 103043, 2023, doi: 10.1016/j.jwpe.2023.103043.
15. T. S. Boopathi, A. Suresh, and R. Rajesh, *"Fe-doped ZnO nanoparticles using Psidium guajava leaf extract,"* Chem. Phys. Lett., vol. 823, p. 140635, 2024, doi: 10.1016/j.cplett.2023.140635.
16. S. N. A. M. Sukri, S. K. Kamarudin, S. M. Zainal Abidin, A. R. Mohamed, and A. M. Nasir, *"Pomegranate-peel-extract-mediated green synthesis of ZnO nanoparticles,"* Arab. J. Chem., vol. 13, no. 3, pp. 2434–2444, 2020, doi: 10.1016/j.arabjc.2019.09.014.
17. L. Kaliraj, R. B. Anbazhagan, A. R. Kannan, and S. Jeyaraj, *"Flower-shaped ZnO nanostructures using Panax-derived panos extract,"* J. Photochem. Photobiol. B, vol. 198, p. 111589, 2019, doi: 10.1016/j.jphotobiol.2019.111589.
18. M. Stan, A. Lung, D. Popa, C. Silipas, and G. I. Popescu, *"Enhanced photocatalytic degradation using ZnO nanoparticles synthesized from plant extracts,"* Mater. Sci. Semicond. Process., vol. 39, pp. 23–29, 2015, doi: 10.1016/j.mssp.2015.04.038.
19. R. Nawaz, M. M. Munir, M. Sohail, M. Bilal, and M. Iqbal, *"Microwave-assisted ionic liquid-based green synthesis of ZnO nanoparticles from Polygonum minus,"* J. Environ. Chem. Eng., vol. 11, no. 6, p. 109970, 2023, doi: 10.1016/j.jece.2023.109970.
20. K. V. Karthik, R. Shwetha, A. R. Raju, N. V. S. S. Raman, and T. M. Srinivasan, *"Synthesis and evaluation of Cu-doped ZnO nanoparticles,"* Mater. Res. Express, vol. 8, no. 4, p. 045503, 2021, doi: 10.1088/2053-1591/abd14b.

21. F. Shah Faisal, M. M. Naseer, A. A. Khan, and A. Khan, *"Bioaugmentation of ZnO nanoparticles via Myristica fragrans fruit extract,"* Arab. J. Chem., vol. 6, no. 11, pp. 1585–1592, 2013, doi: 10.1016/j.arabjc.2013.02.008.
22. G. Yashni, S. Prabha, and D. Chandrasekaran, *"Green synthesis of ZnO nanoparticles using Coriandrum sativum,"* Desalination Water Treat., vol. 163, pp. 84–92, 2019, doi: 10.5004/dwt.2019.24584.
23. T. Bhuyan, P. Khanuja, B. Das, and A. P. Ranjan, *"Neem-leaf-mediated green synthesis of ZnO nanoparticles,"* Adv. Nat. Sci.: Nanosci. Nanotechnol., vol. 6, no. 2, p. 025010, 2015, doi: 10.1088/2043-6262/6/2/025010.
24. P. Priyanka and V. C. Srivastava, *"Photocatalytic oxidation using Fe-doped ZnO,"* Ind. Eng. Chem. Res., vol. 52, no. 50, pp. 17790–17799, 2013, doi: 10.1021/ie401973r.
25. M. S. Vasheghani Farahani, H. Aliakbarzadeh, H. Rezaei, and M. Ghasemi, *"Fe-doped ZnO/nanocellulose nanocomposite for methylene blue degradation,"* Cellulose, vol. 29, no. 13, pp. 7277–7299, 2022, doi: 10.1007/s10570-022-04735-y.
26. F. Wu, J. Zhang, Y. Sun, Z. Liu, and C. Wang, *"Photocatalytic activity of electrospun Fe-doped ZnO nanofibers,"* Environ. Prog. Sustainable Energy, vol. 42, no. 1, pp. 1–12, 2023, doi: 10.1002/ep.13986.
27. G. Dharmana, M. V. L. R. Anitha, M. L. S. Rani, and V. Narayanan, *"Fe-doped ZnO/tin sulfide heterostructures for photocatalysis,"* J. Chem., art. 1407395, 2023, doi: 10.1155/2023/1407395.
28. Y. G. Habba, A. R. Alharbi, and M. A. Bassyouni, *"Enhanced photocatalytic activity of Fe-doped ZnO nanowires,"* Appl. Sci., vol. 7, no. 11, art. 1185, 2017, doi: 10.3390/app7111185.
29. C. B. Ong, P. L. Lim, and B. H. Ng, *"Integrated adsorption-photocatalytic reactor using Fe-doped ZnO,"* Environ. Sci. Pollut. Res., vol. 26, no. 33, pp. 33856–33869, 2019, doi: 10.1007/s11356-018-2557-2.
30. A. Popa, M. Enculescu, and L. C. Nistor, *"Photoluminescence and photocatalytic properties of MWNTs decorated with Fe-doped ZnO,"* Materials, vol. 16, no. 7, art. 2858, 2023, doi: 10.3390/ma16072858.
31. J. Xiao, H. Cheng, Y. Li, J. He, and Y. Zhang, *"Stabilization mechanism of ZnO nanoparticles by Fe doping,"* arXiv preprint arXiv:1401.7180, 2014, doi: 10.48550/arXiv.1401.7180.
32. H.-Y. Chai, L.-Y. Chen, C.-C. Huang, and S.-H. Cheng, *"Green synthesis of Fe-doped*

ZnO via Hibiscus extract," Mater. Lett., vol. 242, pp. 103–106, 2019, doi: 10.1016/j.matlet.2019.01.116.

33. N. Jadon, S. Kumar, A. Kumar, and R. P. Singh, *"Green synthesis of Fe_2O_3/ZnO nanocomposite,"* Curr. Anal. Chem., vol. 20, no. 3, pp. 162–174, 2024, doi: 10.2174/0115734110297844240119062857.
34. A. K. Jha and S. Chakraborty, *"Photocatalytic degradation using nZVI from Shorea robusta,"* Water Sci. Technol., vol. 82, no. 12, pp. 2707–2719, 2020, doi: 10.2166/wst.2020.517.